Oxidation of Metals, Vol. 26, Nos. 3/4, 1986

Oxidation of Commercial Purity Titanium

J. Unnam,* R. N. Shenoy,*† and R. K. Clark‡

Received October 31, 1985; revised January 17, 1986

The oxidation kinetics of commercial purity Ti-A55 exposed to laboratory air in the 593–760°C temperature range were continuously monitored by thermogravimetric analysis. The oxide thickness was measured by microscopy and the substrate contamination was estimated from microhardness measurements. The microhardness depth profiles were converted to oxygen composition profiles using calibration data. The oxygen diffusion coefficient in alpha-Ti appears to be approximately concentration independent in the 1–10 at.% oxygen range. The combination of an "effective diffusion coefficient" and an "effective solubility" at the oxide-metal interface usefully describes the diffusion process over the entire composition range. A model for the total parabolic oxidation kinetics, accounting for the two individual components, oxide growth and solid solution formation, has been proposed. Diffusion coefficient for oxygen in TiO_2 has been estimated as a function of temperature and is found to be about 50 times the value in alpha-Ti. The metallographically prepared cross-sections of the oxidized specimens revealed a "moving boundary" in the substrate, parallel to the oxide-metal interface. This boundary was associated with a specific oxygen level of 5.0 ± 0.5 at.%. It occurred at a distance from the oxide-metal interface which was correlatable with temperature and time of exposure. The diffusion coefficient corresponding to the composition of this moving boundary is in excellent agreement with the effective diffusion coefficient for the substrate contamination.

KEY WORDS: oxidation; titanium; thermogravimetry; microhardness; modeling.

*Analytical Services and Materials, Inc., 28 Research Drive, Hampton, VA 23666.
†Formerly with Vigyan Research Associates, Inc., 28 Research Drive, Hampton, VA 23666.
‡NASA Langley Research Center, Hampton, VA 23665.

0030-770X/86/1000-0231$05.00/0

INTRODUCTION

The oxidation of titanium, in view of its relevance to high temperature applications, has been studied extensively over the last thirty years.[1-11] These studies were largely related to weight gain measurements in a wide range of temperatures and oxidizing atmospheres. The results of these investigations may be broadly grouped as those related to rate laws of oxygen intake and those concerned with mechanisms (formation of oxide and solid solution, nature of the oxide, etc.). Despite the vast body of technical information, the literature appears to be deficient in the following respects:

(i) The delineation of oxide and solid solution contributions to the overall weight gain during the parabolic stage of oxidation has not been clearly dealt with.

(ii) The solubility limit of oxygen in alpha-Ti, as given by the Ti(O) phase diagram,[12] is 34 at.% oxygen (14.5 wt.% O). It is customarily assumed that this level of solubility is quickly reached at the oxide-metal interface during an oxidation exposure. The development of the theoretical solubility limit, however, is expected to be a function of temperature and time, the higher temperatures promoting an earlier attainment of this solubility limit.

(iii) In the diffusion analysis it is assumed that that diffusivity of oxygen is concentration-independent. Considering the fact that oxygen concentration in alpha-Ti varies over a wide range along the diffusion path, there is a need to ascertain whether or not the oxygen diffusivity is indeed concentration independent and, if concentration dependent, how well an "effective" concentration independent diffusivity could still describe the overall diffusion process. In the earlier investigations, the substrate oxygen concentration profiles were incorrectly deduced from microhardness depth profiles. In some investigations,[3] the microhardness number was assumed to be linearly related to wt.% oxygen (with theoretical solubility limit of 14.5 wt.% being directly related to the maximum hardness number obtained for the alloy). In other investigations[8] very limited oxygen-hardness calibration data (oxygen in the range of 0-3 at.%) were utilized to predict the diffusion behavior for the entire range. Diffusion coefficients hitherto reported in the literature are therefore questionable. The present investigation seeks to address all these issues.

LIST OF SYMBOLS

A_s: Area under C_s vs. X profile, at.% oxygen times cm.

C_s: Concentration of oxygen in the alpha-Ti solid solution (see Fig. 1), at.%.

C_z: Concentration of oxygen in the oxide (see Fig. 1), at.%.

D_o: Frequency factor, $cm^2\ sec^{-1}$.
D_s Diffusion coefficient of oxygen in the alpha-Ti solid solution, $cm^2\ sec^{-1}$.
D_z: Diffusion coefficient of oxygen in the oxide, $cm^2\ sec^{-1}$.
erfc: Error function complement.
KHN: Knoop hardness number (subscripts 5 g and 15 g represent indenter loads).
Q: Activation energy for oxygen diffusion in oxide or in solid solution, $cal\ mol^{-1}$.
R: Gas constant, $=1.987\ cal\ mole^{-1}\ deg\ K^{-1}$.
r: Oxide growth constant defined by $z = rt^{1/2}$, $cm\ sec^{-1/2}$.
T: Temperature, K.
t: Time, sec.
W_{if}: Total weight gain per unit area from initial and final weights, $g\ cm^{-2}$.
W_z: Weight gain per unit area due to oxide growth, $g\ cm^{-2}$.
W_{zs}: Total weight gain per unit area due to oxide and solid solution, $= w_z + w_s$, $g\ cm^{-2}$.
X: Distance from oxide-metal interface, cm.
X_{mb}: Distance of the "moving boundary" from the oxide-metal interface, cm.
z: Oxide thickness, cm.

Subscripts

if: Obtained from initial and final weights of specimen.
l: Solubility limit.
mb: Of "moving boundary" in solid-solution.
zs: For the oxide plus solid-solution.
o: Corresponding to base level.
5g: With 5 gram load.
15g: With 15 gram load.

THEORY

The phenomenological aspect of diffusion in a two-phase (oxide-metal) system, during parabolic oxidation, may be described with reference to the Wagner's model.[13] This model has been used to describe the oxidation of Zirconium[14,15] and is expected to be analogous to the oxidation of titanium, in view of (i) similar crystal structures of the metal and the oxide phases (HCP and tetragonal, respectively) for Zr and Ti, (ii) extensive oxygen solid solubility in both metals, and (iii) compact nature of the oxides during parabolic oxidation. Figure 1 shows a schematic display of the oxygen concentration profile in oxidized titanium. It is composed of two individual concentration profiles, one corresponding to the oxide TiO_2 of thickness z

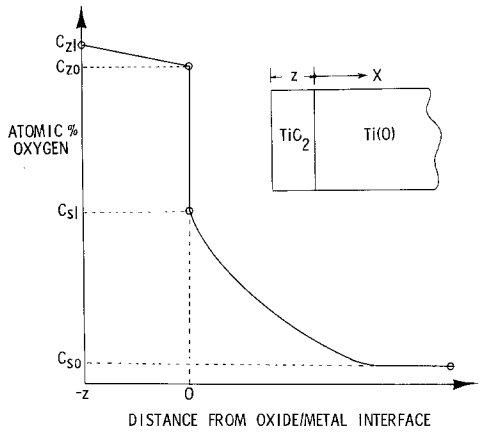

Fig. 1. Schematic of oxygen concentration profile in oxidized titanium.

and the other relating to the substrate which is made up of the solid solution Ti(O). Ti(O) has a large oxygen solubility range extending from C_{sl} at the oxide-metal interface to C_{so} deep within the substrate corresponding to the base oxygen content. C_{sl} is in general a function of exposure time and temperature[16] with 34 at.% as the maximum attainable value.

TiO_2 has a small oxygen solubility range. There are disagreements, however, as to the extent of nonstoichiometry in the oxide. Elliott[17] cites the C_z range to extend from 66.477 to 66.667 at.% corresponding to $TiO_{2-0.017}$ and TiO_2, respectively. Blumenthal and Whitmore[18] estimated the homogeneity range of TiO_{2-y} in the 900–1000°C range to extend to a value of y approximately equal to 0.01. Anderson and Khan[19] quote unpublished results of Steele and Zador[20] at 1000°C which put the value of y at 0.008. The nonstoichiometry data presented by Kofstad[21] correspond to very low oxygen partial pressures and high temperatures, and if extrapolated to atmospheric pressure and present temperature range would result in a value of about 0.001 for y.

In view of the small range of oxygen solubility in the oxide phase, it may be assumed that the diffusion coefficient of oxygen in the oxide (D_z) is independent of composition and also that the concentration gradient within the oxide is linear. The oxygen concentration in the oxide (C_z) is then given by

$$C_z = C_{zo} - (X/z)(C_{zl} - C_{zo}) \tag{1}$$

Assuming that the diffusion coefficient, D_s, is concentration independent, the solution of Fick's II law for the concentration in the solid solution

is given by[22]

$$C_s = C_{so} + (C_{sl} - C_{so})\ erfc(X/2(D_s t)^{1/2}) \tag{2}$$

The oxide thickness can be determined by the interface flux-balance equation

$$(C_{zo} - C_{sl})(dz/dt) = -D_z(dC_z/dX) + D_s(dC_s/dX)_{x=0} \tag{3}$$

By postulating a parabolic growth law for the oxide,

$$z = rt^{1/2} \tag{4}$$

where r is a constant for a given temperature, Eq. (3) reduces to

$$r = -p(D_s/\pi)^{1/2} + (p^2 D_s/\pi + 2qD_z)^{1/2} \tag{5}$$

where $p = (C_{sl} - C_{so})/(C_{zo} - C_{sl})$ and $q = (C_{zl} - C_{zo})/(C_{zo} - C_{sl})$. Equation (5) can be used to calculate D_z if the oxide thickness, solubility limits in the oxide and the solid solution, and D_s are known.

An oxidation model for Ti, based on weight gain, may be viewed as being composed of two basic components—oxide growth and solid solution formation, which are described by Eqs. (1), (2), and (5). For TiO_2 (rutile) which has a density[23] of 4.26 g/cm^3 and weight fraction oxygen of 0.40. The weight gain for unit area due to oxide growth is given by

$$W_z = 1.704z \tag{6}$$

and by virtue of Eq. (4)

$$W_z = 1.704rt^{1/2} \tag{7}$$

The area under the concentration profile in the solid solution, A_s, is given by the integration of Eq. (2) over the limits X = zero to infinity. Thus,

$$A_s = 2(C_{sl} - C_{so})(D_s t/\pi)^{1/2} \tag{8}$$

A_s represents the mass of oxygen diffused into the substrate and has the units of at.% oxygen times cm. In order to obtain W_s, the weight gain per unit area due to solid-solution formation in terms of g/cm^2, it is necessary to represent the ordinate of the concentration profile (prior to integration) in terms of grams of oxygen per cm^3 rather than at.% O. This is accomplished by converting at.% O into weight fraction O and then multiplying by the corresponding density of the Ti(O) solid solution. The use of a single conversion factor permits analytical evaluation of the integral and results in a sufficiently accurate value for W_s. That is

$$W_s = 2f(C_{sl} - C_{so})(D_s t/\pi)^{1/2} \tag{9}$$

where f is a constant multiplier that converts the area under a concentration profile from at.% oxygen times cm into g/cm^2. The total weight gain per unit area of specimen, W_{zs}, is obtained by using Eqs. (7) and (9).

$$W_{zs} = W_z + W_s \tag{10}$$

Table I. Chemical Composition (wt.%) of Ti-A55 Sheet and Foil

Alloy \ Element	Fe	H	C	N	O	OET[a]	Ti
Ti-A55 Sheet	0.18	0.01	0.02	0.01	0.14	<0.4	Bal
Ti-A55 Foil	0.19	—	0.02	0.03	0.10	<0.4	Bal

[a]Other elements total.

EXPERIMENTAL PROCEDURE

Specimens

Titanium specimens, 0.308 cm × 1.5 cm × 1.5 cm with a nominal surface area of 6.3 cm^2, were fabricated from a commercial purity Ti-A55 sheet. The samples were thoroughly degreased in a soap solution followed by soaking in acetone. They were then annealed for 100 hr at 871°C (below the beta-transus) in a vacuum better than 7×10^{-7} torr in order to obtain a reference microstructure so that grain-size would not change during subsequent oxidation exposures. The average grain-size was approximately 130 μm. This coarse grain-size also enabled the microhardness measurements to be performed wholly inside an individual grain of oxidized sample, so that grain orientation effect on hardness was eliminated within a given scan. The vacuum annealed specimens were acid-cleaned in a Kroll's solution (3% HNO_3 + 2% HF + 95% H_2O) for 15 sec to give a bright, shiny surface. The oxygen plus nitrogen content of vacuum annealed specimens was chemically analyzed to be 0.15 wt.% (Table I).

Exposure Apparatus

The oxidation exposures were performed in a thermogravimetric analysis unit (TGA) in laboratory air at about 50% relative humidity. The TGA unit consisted of a vertical tube furnace, a Cahn-Ventron electrobalance for continuous monitoring of specimen weight and a HP85 computer for data collection. Weight gains were measured with a sensitivity of 10 μg over the entire temperature range. Temperature measurements were accurate to 1°C.

Ti(O) Standards and Metallography

In order to obtain oxygen composition profiles from microhardness depth profiles, Ti(O) solid solution standards were prepared in the following manner. Several 0.005 cm thick Ti-A55 foils having 0.13 wt.% oxygen plus nitrogen (Table I) were oxidized in laboratory air for different lengths of

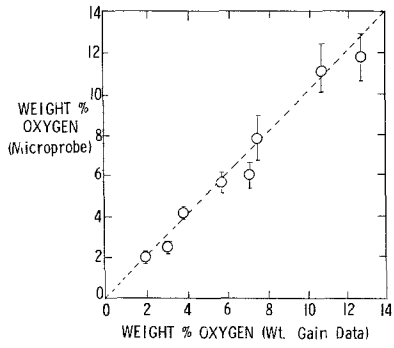

Fig. 2. Surface composition determined from electron microprobe plotted as a function of bulk composition determined from initial and final weights.

time at 855°C to absorb different amounts of oxygen. These were subsequently homogenization annealed at 871°C for 120 hr in a vaccum better than 7×10^{-7} torr. The vacuum annealing heat treatment increased the specimen weights marginally (by 0.05-0.40%) indicating an acceptable level of vacuum during heat treatment. The above standards, representing a range of oxygen levels from about 0.2 to 12 wt.% were analyzed by electron microprobe for surface composition. The resulting oxygen compositions were in excellent agreement with those deduced from the specimen weights before oxidation exposure and after homogenization anneal (Fig. 2). Wavelength scans in the microprobe did not reveal the presence of nitrogen

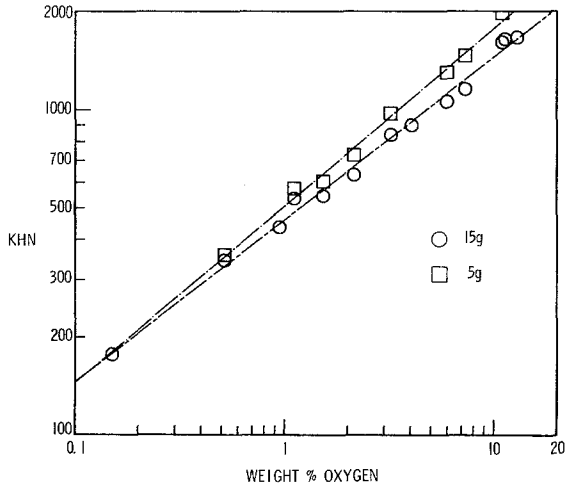

Fig. 3. Calibration of microhardness with oxygen weight percent in Ti-A55.

in the standards. Cross-sections of these standards were prepared for metallography. No trace of TiO_2 was detected. Thus the wt.% O at the end of vacuum annealing truly represents the oxygen content in solid solution. At least 15 to 20 Knoop indentations were made on each of the standards employing both a 15 g and a 5 g load. The microhardness versus wt.% oxygen calibration data are shown in Fig. 3.

Cross-sections of the oxidized specimens were prepared for metallography using Kroll's reagent (2% HNO_3+1% HF+97% H_2O). The specimens were copper-coated (30 μm) prior to metallographic preparation, in order to preserve the surface oxide. Microhardness depth profiles were obtained from the cross-sections, employing a 15 g load and a Knoop indenter. The optics in the microhardness tester enabled the measurements of the long diagonal of the hardness impressions and also the oxide thickness to ±0.1 μm. Oxide thickness measurements were also performed in a scanning electron microscope.

RESULTS AND DISCUSSION

Total Weight Gain

Figure 4 shows typical apparent weight gain data for the 649°C exposure, plotted as a function of the square root of time (solid line). During the time taken to heat the specimen from room temperature to 649°C, the specimen experiences a true weight gain due to oxidation and an apparent weight loss due to buoyancy forces of the heated air. The buoyancy effects

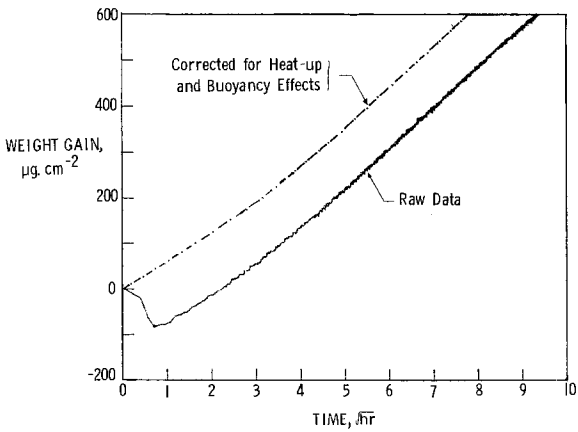

Fig. 4. Raw and corrected thermogravimetric data for Ti-A55 at 649°C.

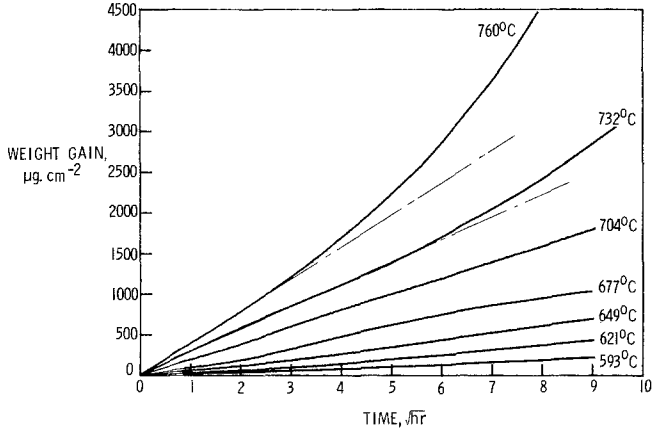

Fig. 5. Weight-gain as a function of square root of time for Ti-A55 oxidized at different temperatures.

were constant for the exposure time beyond the initial 0.5 hr. The transient temperature effects on weight gain also lasted about 0.5 hr. Thus the exposures were truly isothermal beyond about 0.5 hr. The corrections due to the combined effect of buoyancy and transient temperature were applied so as to obtain the true weight gain (broken line). The true weight gain curve passes through the $t = 0$ origin and has two distinct slopes; an initial slope (for the 649°C exposure) until $t \simeq (2.5)^2$ hr and a slightly higher slope thereafter. A parallel investigation using an X-ray technique ascribes the change of slope in weight gain to an increase in oxygen solubility level at the oxide-metal interface.[16] The time at which the initial slope changes is influenced by exposure temperature, with higher temperatures promoting shorter times.

Figure 5 shows true weight gain as a function of square root of time for the 593–760°C range of oxidation exposures. The total oxidation rate in the 593–704°C range for up to 100 hr is essentially parabolic with respect to time, indicating weight gains due to oxide growth and solid solution to be individually parabolic. The 732 and 760°C exposures have a parabolic stage up to only about 30 and 10 hr, respectively.

Oxide Growth

X-ray diffraction studies on the oxidized specimens revealed the oxide to be entirely rutile. Figure 6 shows a plot of normalized oxide thickness, r, as a function of inverse temperature. A linear regression gives

$$r = z/t^{1/2} = 1.5 \exp(-27{,}350/(RT)) \tag{11}$$

where 27,350 cal/mole is the activation energy for the growth of oxide. The

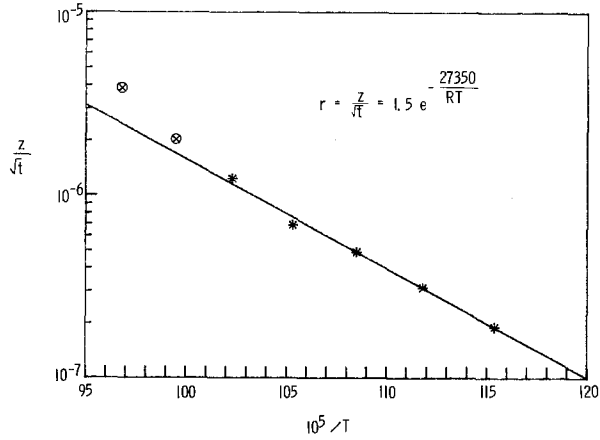

Fig. 6. Variation of scaled oxide thickness as a function of inverse temperature. The circled crosses are not used in obtaining the best-fit straight line because oxide growth for these specimens may not be entirely parabolic.

data points corresponding to 732 and 760°C were not used in the above regression because the oxide growth kinetics for these temperatures may not be wholly parabolic over the entire exposure time.

Equation (11) enables prediction of oxide thickness and also evaluation of weight gain per unit area due to oxide growth, W_z, through Eq. (6). While the activation energy for the growth of oxide as given by Eq. (11) is empirical in nature, that associated with either D_s or D_z in Eq. (5) has fundamental significance.

Solid Solution Formation

Hardness depth profiles for different grains showed different base hardness values typifying grain orientation effects on the mechanical properties of an anisotropic material. In view of this, a $KHN_{15\,g}$ of 180 (which was the average of hardness numbers for more than 40 grains in an unexposed specimen with a uniform oxygen plus nitrogen content of 0.15 wt.%) was used as the datum hardness number for normalizing all the hardness profiles. The calibration data in Fig. 3 was then used to obtain oxygen composition profiles. A 5 g load was also used in order to obtain the hardness data from regions as close to the oxide-metal interface (about 2 μm) as was physically possible. The 5 g calibration data in Fig. 3 were used to compute the compositions from the $KHN_{5\,g}$ data.

From the a and c lattice parameter data for Ti(O) solid solutions,[4] it was estimated that the density of Ti(O) solid solution varied over a range

Table II. Weight-Gain Data for Oxidized Ti-A55 Specimens

Temp °C	Time hr	W_z^a	W_s^a	W_{zs}^a	W_{if}^a	(W_s/W_{zs})
593	96.9	193	83	276	246	0.30
621	95.8	314	151	465	472	0.32
649	89.2	474	218	692	730	0.32
677	94.4	683	383	1066	1080	0.36
704	92.2	1208	554	1762	1880	0.31
732	96.1	2195	816	3011	3180	0.27
760	64.4	3176	1144	4320	4430	0.26

[a] In units of $\mu g \cdot cm^{-2}$.

of 4.52–5.04 g cm^{-3} (corresponding to 0–14.5 wt.% oxygen). In order to compute the weight-gain per unit area due to solid solution formation, W_s, a given composition in weight fraction oxygen ordinate was multiplied by the corresponding density of the Ti(O) solid solution and the product was integrated over the entire diffusion distance in the profile. Table II lists W_s along with W_z for the various exposures. The following may be inferred from Table II.

(a) Weight gains obtained from the initial and final weights (W_{if}) closely approximate those estimated from the individual components of oxidation ($W_z + W_s$), testifying to a high degree of internal consistency of independent measurements between vastly different techniques (microbalance, microscopy, and microhardness).

(b) In view of the closeness of values of W_{zs} (estimated from the theoretical density of pore-free oxide) and W_{if}, the existence of porosity in the oxide scale, at least in the time-temperature domain considered in the present study, does not appear to be likely. Although the 760°C exposure is associated with a linear oxide growth (subsequent to the initial parabolic stage), it would appear that the oxide scale is still relatively free of porosity.

(c) The ratio of oxygen diffused into the matrix to the total oxygen pick-up is approximately 0.31 ± 0.05 for the entire range of temperatures (including 760°C). The ratio of 0.26 for 760°C compares favorably with 0.29 for 750°C reported by Gomes.[11]

Moving Boundary

The metallographically prepared cross-sections of the oxidized specimens revealed a "moving boundary" in the alpha-matrix, which was parallel to the oxide-metal interface. Figure 7 is an SEM micrograph of the cross-section of a metallographically prepared 649°C specimen. The following observations are made based on this and other specimens:

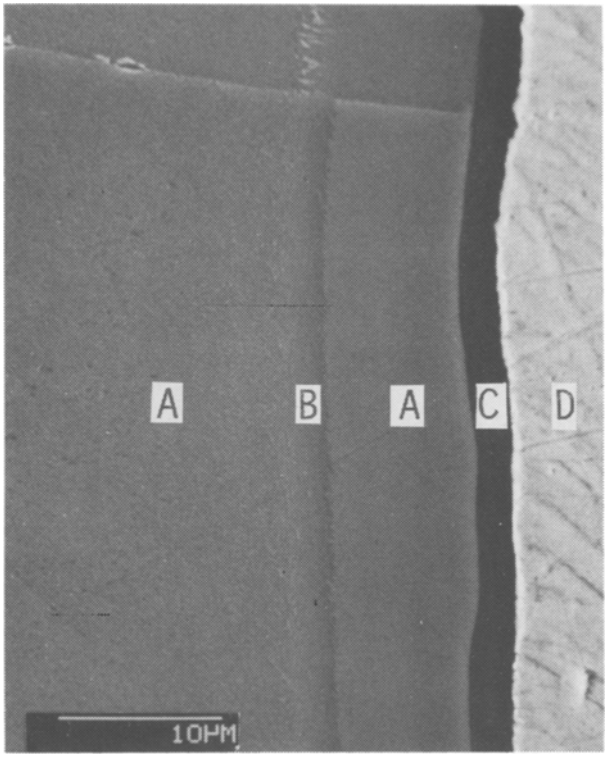

Fig. 7. SEM micrograph of Ti-A55 oxidizied at 649°C for 65.9 hr. A = matrix, B = moving boundary, C = oxide, and D = copper coating.

(i) The moving boundary represents a demarcation between the relatively oxygen-rich and the oxygen-poor regions of the Ti(O) matrix. However, the microhardness data does not indicate any discontinuity in composition across this boundary.

(ii) The distance, X_{mb}, of the moving boundary from the oxide-metal interface has a definite correlation with time and temperature of exposure (Table III). The higher the temperature or the longer the exposure time, the larger the value of X_{mb}.

(iii) Composition of the moving boundary (Table III) as given by the composition profiles for the various temperatures is 5.0 ± 0.5 at.% O. It appears that the etching reaction is sensitive to the composition dependent electrochemical differences in the Ti(O) matrix at this oxygen value, bringing about a marked optical contrast between the oxygen-rich and oxygen-poor regions across the boundary.

Table III. Data on the "Moving-Boundary" in Oxidized Ti-A55 Specimens

Temp. °C	Time hr	X_{mb} μm	KHN_{5g} at X_{mb}	C at X_{mb} at.% O	$D_s \times 10^{13}$ $cm^2 \cdot sec^{-1}$
593	96.9	3.9±0.3	587	4.7	1.4
621	95.8	6.9±0.7	591	4.8	4.6
649	89.2	11.6±1.0	573	4.5	13.0
677	94.4	16.8±1.0	626	5.3	31.0
704	92.2	29.1±1.5	626	5.3	97.0
732	96.1	38.3±1.7	609	5.1	152.0
760	64.4	43.3±2.1	630	5.4	308.0

It must be emphasized that the presence of the moving boundary in the air-oxidized specimens in the temperature range studied was a definite and a consistent observation. Allusion to such a moving boundary was first made by Kofstad[5] although no quantitative data in relation to its location in the alpha solid solution were presented.

Oxygen Concentration at Oxide-Metal Interface

It is customarily assumed that during the course of an oxidation exposure, the saturation limit of 34 at.% oxygen in the alpha solid solution is reached immediately at the oxide-metal interface. However, Jenkins[2] determined that after a heating period lasting 72 hr, the interface oxygen composition did not exceed 12 at.% at 650°C, 19 at.% at 800°C, and 25 at.% at 900°C. Hurlen[7] observed that in the temperature range of 650–700°C, oxygen dissolved readily with an initial surface concentration of 14–15 at.% rather than with a higher concentration because Ti_6O (corresponding to 14.3 at%) was a more stable phase in the initial stages than other oxides in the Ti-O system. While Kofstad *et al.*[24] noted the apparent solubility at the oxide-metal interface not to exceed 25 at.%, Wiedemann[25] and David *et al.*[26] obtained a value of 20 at.%. The most recently reported values of C_{s1} are those due to Wiedemann and Unnam,[16] who on the basis of X-ray diffraction studies on oxidized Ti, observed the interface solid solubility levels to vary from an initial lower value of 20 at.% to subsequent higher values of 25 at.% and 34 at.%.

The concentration profile for the Ti(O) solid solution is given by Eq. (2). The attainment of 34 at.% oxygen for C_{sl} is, in general, a function of temperature and time of exposure. While it would not be expected to be attained for the 593°C exposure even at the end of 100 hr, it would have a reasonable chance of being achieved for the 760°C exposure in a much shorter time. The use of a 5 g load in the hardness measurement enabled

the estimation of oxygen compositions at distances as close as 1.5-2 μm from the oxide-metal interface. Even though the composition varied steeply near the interface, it was felt useful to linearly extrapolate the composition profile to the interface. This resulted in the determination of C_{sl} for the various exposures. The C_{sl} for the temperature range 593-677°C was 20 at.% oxygen while the value for the 760°C exposure was close to the theoretical solubility limit of 34%. The 732°C exposure had a value of about 25%. The values of C_{sl} obtained in the present investigation, thus are in excellent agreement with those obtained earlier.[16,24-26]

Diffusion Coefficient of Oxygen in Alpha-Ti

The concentration profile for the Ti(O) solid solution is given by Eq. (2). Equation (2) is rigorous only when C_s, C_{so}, and C_{sl} are all expressed as true concentrations, that is, in units of number of atoms of diffusing species per unit volume. The use of wt.% O for concentration appreciably distorts the form of Eq. (2) in view of the nonlinear relationship between wt.% O and atoms per unit volume. The failure to recognize this fact leads to spurious diffusion data. The use of at.% for concentration is more appropriate under the circumstance. The concentration profiles (with at.% O representing concentration) are shown in Fig. 8 at 2.5 μm depth intervals.

Although an actual concentration profile is characterized by a C_{sl} which itself is dependent on time and temperature of exposure, it seems relevant

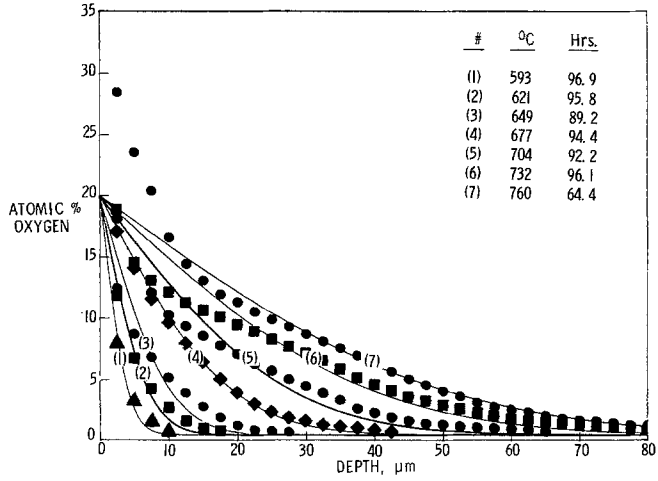

Fig. 8. Oxygen depth profiles for various exposures deduced from microhardness data. The symbols represent experimental data while the curves represent best-fits using Eq. (2) and $C_{sl} = 20$.

to investigate how best one appropriate value of C_{sl} (together with a concentration-independent D_s) satisfactorily describes the concentration profiles in the time-temperature domain under consideration. In light of the above, it is apparent from Fig. 8 that just one value for C_{sl}, namely 20 at.%, suffices to satisfactorily describe all the concentration profiles excepting those corresponding to the 732°C and the 760°C exposures. In an effort to appreciate how significant the dependence of D_s on concentration is, Eq. (2) has been used as a "yardstick." Diffusion coefficients were computed using Eq. (2) with $C_{sl} = 20$ and $C_{so} = 0.44$, and are shown in Fig. 9. D_s increases sharply below about 1 at.% O while it decreases steeply above about 10 at.% O, and it is approximately constant in the 1-10 at.% range. Thus the use of Eq. (2) indicates a composition range on either side of which D_s is strongly concentration dependent. Within this composition range however, D_s is fairly independent of concentration. Also, a correct qualitative trend in the variation of D_s with C is seen outside the 1-10 at.% range. The diffusion coefficients were obtained by the following three methods.

Method A: Fitting the Concentration Profile

It is apparent from Fig. 8 that the bulk of the concentration profile for every exposure temperature is confined within the 1-10 at.% O range for which the estimation of a concentration independent D_s seems appropriate.

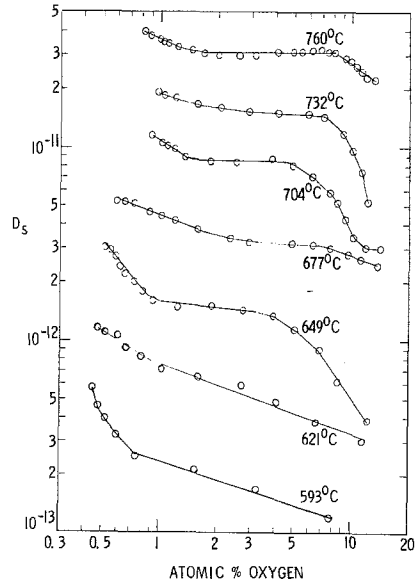

Fig. 9. Diffusion coefficients for Ti(O) system as a function of at.% oxygen for various temperatures.

Optimization techniques were therefore used to obtain a single D for every temperature based on Eq. (2) such that it fit the experimental data below 10 at.% oxygen. The resulting diffusion coefficients are listed in Table IV. The best-fit concentration profiles are shown superimposed as lines on the actual concentration profiles in Fig. 8. It may be seen that the constant D fits the data very well for the 593–704°C exposures (dilute solutions). The fit beyond 10 at.% O for the 732 and 760°C exposures is not completely satisfactory because of the strong concentration dependence of D_s and the actual existence of a higher solubility than the assumed C_{sl} of 20 in generating these fits. In this context, the $C_{sl} = 20$ may be regarded as an effective C_{sl} since it, in combination with a concentration independent D_s, usefully described the diffusion behavior for dilute Ti(O) solutions (<10 at.% O).

Method B: From Area Under the Concentration Profile

The area under the concentration profile, Ag, is given by Eq. (8). Table V lists A_s (deduced from hardness profiles), and the D_s calculated using Eq. (8). This calculation thus assumes a concentration independent diffusion coefficient, $C_{sl} = 20$, and an error function concentration profile that has the same area as the actual concentration profile. The values of D_s so estimated may be regarded as effective diffusion coefficients.

Method C: From the Moving Boundary

Corresponding to the location and oxygen composition of the moving boundary, values of D_s were computed from Eq. (2) with $C_{sl} = 20$ and $C_{so} = 0.44$. The results are listed in Table III.

A comparison of the D_s's in Tables III and V reveals that the D_s's obtained from the moving boundary and those from the area under the

Table IV. Diffusion Coefficients for Oxygen in Alpha-Ti Based on Fitting of the Hardness Deduced Concentration Profile (Below 20 at.% O) by Eq. (2) with $C_{sl} = 20$ and $C_{so} = 0.44$

Temp. °C	time hr	$D_s \times 10^{13}$ $cm^2 \cdot sec^{-1}$
593	96.9	1.4
621	95.8	4.1
649	89.2	9.3
677	94.4	31.0
704	92.2	64.0
732	96.1	128.0
760	64.4	298.0

Table V. Diffusion Coefficients from Area Under the Concentration Profile

Temp. °C	Time hr	A_s at.% O × cm	$D_s \times 10^{13}$ $cm^2 \cdot sec^{-1}$
593	96.9	0.0048	1.4
621	95.8	0.0085	4.3
649	89.2	0.0120	9.2
677	94.4	0.0220	30.0
704	92.2	0.0320	64.0
732	96.1	0.0456	124.0
760	64.4	0.0621	341.0

concentration profiles are very similar. In other words, the effective D_s, which is supposed to be representative of the entire concentration range, is closely identified by the composition of the moving boundary (which has an average value of 5.0 ± 0.5 at.% O). Reliable diffusion coefficients could therefore readily be obtained by simply noting the position of the moving boundary (in relation to time and temperature of exposure) and its composition. Thus, the experimental observation of the moving boundary seems to be of immense practical utility in the study of titanium oxidation.

In view of the close agreement between the D_s's estimated by the above three methods, a single plot of variation of D_s with inverse temperature is shown in Fig. 10. A linear regression gives

$$D_s = 50 \exp(-57{,}600/(RT)) \tag{12}$$

where 57,600 cal/mole is the activation energy for the diffusion of oxygen in alpha-Ti.

Although the methods A and B for computation of D_s's are based on the concentration profile, method C is truly independent of the other two with the *proviso* that the same value of 20 at.% O for the effective C_{sl} and a concentration independent D_s are assumed for all the three methods. Since the agreement between each of these methods is excellent, it is appropriate to say that, in the time-temperature domain under consideration, oxygen diffusion in alpha-titanium may be adequately described by a concentration independent D_s. With the help of these D_s's and the effective C_{sl} of 20, the bulk of the concentration profiles may be generated for all the exposures under consideration.

Table VI summarizes the D_s at 677°C (the temperature corresponding to the average of 593–760°C range employed in the present investigation) for Zr, Hf, and Ti, computed on the basis of equations available in the literature.[14,27,28] It is evident that the agreement between the absolute values of D_s for Zr, Hf, and Ti is excellent, as is to be expected.

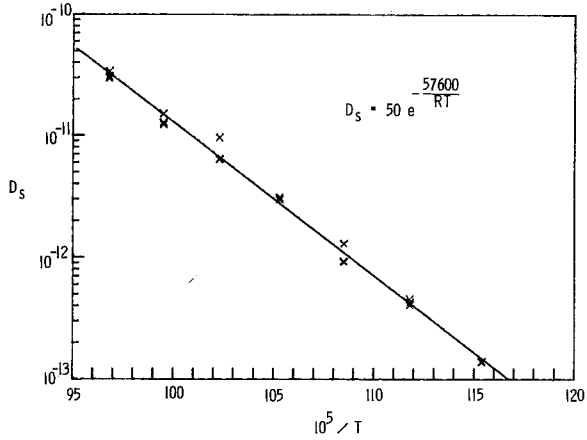

Fig. 10. Diffusion coefficients for oxygen in alpha-Ti obtained by three different methods from the concentration profiles deduced from microhardness measurements on the specimen cross-sections.

Diffusion Coefficients for Oxygen in TiO_2 (Rutile)

Diffusion coefficients for oxygen in TiO_2, D_z, were calculated from Eq. (5), using r and D_s obtained from Eqs. (11) and (12). They are listed in Table VII together with r, D_s, and D_z/D_s. As can be seen, D_z is about 50 times that of D_s for the entire (593–760°C) temperature range. A plot of D_z as a function of inverse temperature is shown in Fig. 11, giving

$$D_z = 870 \exp(-55{,}535/(RT)) \tag{13}$$

where 55,535 cal/mole is the activation energy for the volume diffusion of oxygen in rutile in the presence of an assumed oxygen gradient in the oxide due to non-stoichiometry; and is quite distinct from the 27,350 cal/mole (Eq. 11) which is the activation energy for oxide growth. Furthermore, the

Table VI. Comparison of Oxygen Diffusion Coefficients at 677°C in Alpha Phases of Zr, Hf, and Ti

Phase	D_o $cm^2 \cdot sec^{-1}$	Q cal mol^{-1}	$D_s \times 10^{13}$ $cm^2 \cdot sec^{-1}$	Ref
Zr	224	59,700	41	14
Hf	30	58,000	14	27
Ti	0.778	48,600	39	28
Ti	50	57,600	28	This paper

Table VII. Calculated Diffusion Coefficients for Oxygen in TiO_2

Temp. °C	$r \times 10^6$	$D_s \times 10^{13}$	$D_z \times 10^{13}$	D_z / D_s
593	0.19	1.5	86	57
621	0.31	4.2	233	55
649	0.49	11.1	595	54
677	0.76	27.8	1440	52
704	1.15	66.2	3320	50
732	1.70	150.0	7320	49
760	2.45	326.0	15,400	47

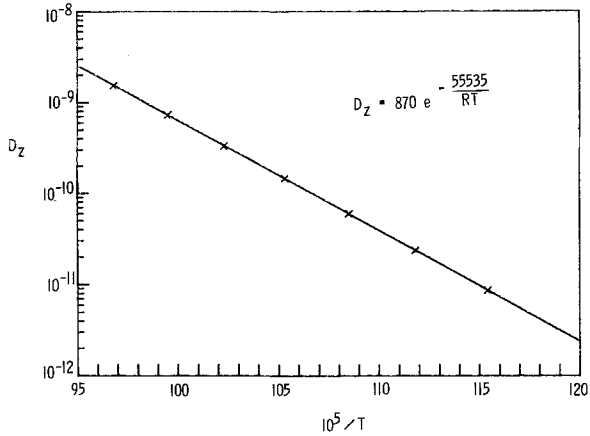

Fig. 11. Diffusion coefficients for oxygen in TiO_2 calculated using Eqs. (5) and (11) with $C_{zl} = 66.667$, $C_{zo} = 66.477$, $C_{sl} = 20$, and $C_{so} = 0.44$.

Table VIII. Comparison of Oxygen Diffusion Coefficient at 677°C in ZrO_2 and TiO_2

Phase	D_o $cm^2 \cdot sec^{-1}$	Q $cal \cdot mol^{-1}$	$D_s \times 10^{13}$ $cm^2 \cdot sec^{-1}$	Ref.
ZrO_2	0.00105	29,300	191	14
TiO_2	870	55,555	144	This paper

Table IX. Experimental Data and Model Predictions for z and W_s

Temp. °C	Time hr	z, μm		W_s, $\mu g \cdot cm^{-2}$	
		Pred.	Exp.	Pred.	Exp.
593	96.9	1.11	1.13	89	83
621	95.8	1.82	1.84	149	151
649	89.2	2.80	2.78	235	218
677	94.4	4.47	4.01	384	383
704	92.2	6.59	7.09	579	554
732	96.1	9.96[a]	12.88	893	816
760	64.4	11.82[a]	18.64	1081	1144

[a] Lower than experimental value because the oxide growth for this exposure is not entirely parabolic.

evaluated value of D_z depends to a large extent on the accuracy with which C_{zo} is known.

D_z at 677°C for oxygen diffusion in ZrO_2 and TiO_2 are compared in Table VIII. It is clear that the absolute values of D_z for these two oxides compare favorably; the agreement betwen the corresponding D_o and Q, is however, not satisfactory.

Weight Gain Model for Ti Oxidation

The weight gain model for oxidation for Ti-A55 may be summarized as follows. The weight gain due to oxide growth is predicted by Eq. (7) where the parabolic growth constant r is given by Eq. (11). Therefore

$$W_z = 2.56 \exp(-27{,}350/(RT))t^{1/2} \tag{14}$$

The weight gain due to solid solution formation is predicted by Eq. (9) where D_s is given by Eq. (12), and f equals $.0178 \pm .0005$ for the present investigation . Therefore

$$w_s = 2.78 \exp(-28{,}800/(RT))t^{1/2} \tag{15}$$

The total weight gain W_{zs} is simply equal to $W_z + W_s$. Table IX lists the weight gains obtained experimentally and those predicted from the oxidation model. The agreement is good for all cases where the oxide is parabolic.

CONCLUSIONS

The following conclusion are drawn based on thermogravimetric, microhardness, microscopy, and diffusion analyses of Ti-A55 specimens exposed to temperatures from 593-760°C in laboratory air for up to 100 hr.

1. The weight-gain due to oxide growth and solid solution formation are essentially parabolic with respect to time. The oxide growth tends to become linear during long exposures at 732 and 760°C.

2. The oxygen diffusion coefficient in Ti(O) is approximately independent of concentration in the 1-10 at.% oxygen range.

3. A concentration independent diffusion coefficient, in combination with an effective solubility limit of 20 at.% O at the oxide-metal interface, usefully describes the diffusion process in the matrix over the entire composition range.

4. The position of of the optically evident moving boundary in the alpha-matrix can be used to estimate oxygen diffusion coefficients in Ti(O). The moving boundary has a composition of 5.0 ± 0.5 at.% oxygen.

5. Activation energies for the diffusion of oxygen in the TiO_2(rutile) and Ti(O) are 55,535 cal/mole and 57,600 cal/mole, respectively. The diffusion coefficient of oxygen in the oxide is about 50 times that of oxygen in Ti(O).

ACKNOWLEDGMENT

Support from the Langley Research Center, National Aeronautics and Space Administration, is appreciated by the authors.

REFERENCES

1. P. H. Morton and W. M. Baldwin, *Trans. Amer. Soc. Met.* **44**, 1004 (1952).
2. A. E. Jenkins, *J. Inst. Met.* **82**, 213-221 (1953-1954).
3. J. E. Reynolds, H. R. Ogden, and R. I. Jaffee, *Trans. ASM* **49**, 280-299 (1957).
4. S. Andersson, B. Collen, U. Kuylenstierna, and A. Magneli, *Acta. Chem. Scand.* **11**, 1641-1652 (1957).
5. P. Kofstad, K. Hauffe, and H. Kjollesdall, *Acta. Chem. Scand.* **12**(2), 239-266 (1958).
6. J. Stringer, *Acta. Met.* **8**, 758-766 (1960).
7. T. Hurlen, *J. Inst. Met.* **89m**, 128-136 (1960-1961).
8. C. E. Shamblen and T. K. Redden, *The Science, Technology and Application of Titanium*, R. I. Jaffee and N. E. Promisel, eds. (Pergamon Press, New York, 1968), pp. 199-208.
9. C. J. Rosa, *Metall. Trans.* **1**, 2517-2522 (1970).
10. L. E. Dunbar, A. F. Mills, G. H. Burghart, and R. M. Clever, 2nd AIAA/ASME Thermophysics Conf., 1978, Paper No. 78-867.
11. J. E. L. Gomes and A. M. Huntz, *Oxid. Met.* **14**(6), 471-498 (1980).
12. M. Hansen, *Constitution of Binary Alloys*, 2nd edition (McGraw-Hill Book Company, New York, 1958), p. 1069.
13. C. Wagner, *Diffusion in Solids, Liquids, Gases*, W. Jost, ed. (Academic Press, New York, 1952), p. 71.
14. J. Debuigne and P. Lehr, *Rev. Met.* **60**, 911 (1963).
15. G. R. Wallwork, W. W. Smeltzer, and C. J. Rosa, *Acta Met.* **12**, 409 (1964).
16. K. E. Wiedemann and J. Unnam, An X-Ray Diffraction Study of Titanium Oxidation, TMS-AIME Paper No. F84-14, 1984.
17. R. P. Elliott, *Constitution of Binary Alloys*, First Supplement (McGraw-Hill Book Company, New York, 1965), p. 697.
18. R. N. Blumenthal and D. H. Whitmore, *J. Electrochem. Soc.* **110**, 92 (1963).

19. J. S. Anderson and A. S. Khan, *J. Less-Common Met.* **22**, 219 (1970).
20. B. C. H. Steele and S. Zador, Ph.D. Thesis (S. Zador) University of London, 1969.
21. P. Kofstad, *Nonstoichiometry, Diffusion, and Electrical Conductivity in Binary Metal Oxides* (Wiley Interscience, New York, 1972), pp. 141.
22. J. Crank, *The Mathematics of Diffusion* (Oxford University Press, London, 1964).
23. Robert C. Weast, ed., *Hand Book of Chemistry and Physics*, 52nd edition (The Chemical Rubber Company, Cleveland, OH, 1971–1972), p. B–150.
24. P. Kofstad, P. B. Anderson, and O. J. Krudtaa, *J. Less-Common Met.* **3**, 89–97 (1961).
25. K. E. Wiedemann, MS Thesis, Virginia Polytechnic Institute and State University, 1983.
26. D. David, E. A. Garcia, X. Lucas, and G. Beranger, *C.R. Acad. Sc., Paris* **t.287**, 125–128 (1978).
27. E. Bisogni, G. Mah, and C. Wert, *J. Less-Common Met.* **7**, 197 (1964).
28. C. J. Rosa, *Metall. Trans.* **1**, 2517–2522 (1970).